

Coherent Detection with an Asynchronous Geiger Mode Array

Joseph C. Marron, Maurice J. Halmos and Brian F. Boland

Raytheon Space and Airborne Systems
2000 E. El Segundo Blvd
El Segundo, CA 90245
joseph.marron@raytheon.com

Abstract

Large format arrays of coherent detectors enable several advanced EO sensing modes including aperture synthesis, turbulence compensation and velocity sensing. Coherent detector arrays that operate in a linear mode are desirable; however, they are often impractical because read-out'ss offering sufficient pixel density and A/D rates are not available. Photon-counting coherent detector arrays based on Geiger-mode Avalanche Photo-Diode (GmAPD) arrays are attractive because they offer large array format, and the output is digitized via the photon arrival times. Furthermore, asynchronous GmAPD arrays offer improved blocking efficiency which in turn improves the frequency fidelity. In fact, the response time of an asynchronous GmAPD macropixel exceeds the reset time of the individual detectors. In this paper we present the results of analysis, modeling and experiments that show the performance levels attainable with asynchronous GmAPD arrays.

1 Analysis of Coherent Detection with Photon-Counting Array

For coherent detection with a photon-counting array, a sub-array of pixels (a macro-pixel) is typically used to detect the signal over a coherence cell. This improves the blocking efficiency caused by the finite pixel reset time. With a traditional coherent detector the detector size is matched to the coherence cell size, $\lambda f/D$, where f is focal length, λ is wavelength, and D is the receiver diameter. For the photon-counting case, we use an array of $M \times M = N_0$ pixels comprising a macro-pixel to cover the coherence cell. An expression for the blocking efficiency is given by [1, 2]

$$B = 1 / \left(1 + T_R \left(\frac{(N_S + N_{LO})^{PDE}}{CPI \cdot N_0} + DCR \right) \right). \quad (1)$$

An expression for the CNR that includes the blocking efficiency is then

$$CNR = \frac{PDE \cdot B \cdot \eta_{HET} N_S N_{LO}}{N_S + N_{LO} + N_0 \cdot B \cdot CPI \cdot DCR / PDE}. \quad (2)$$

It follows that because $B < 1$ in practice, the performance of the asynchronous GmAPD is always less than that of a conventional linear mode coherent detector; however, the large formats and high-bandwidths achievable with asynchronous GmAPDs can offset this for many cases. Also note that for a linear mode detector optimal performance is obtained with N_{LO} much greater than N_s , whereas for a Geiger mode detector N_{LO} must be limited to keep the blocking efficiency high.

Figure 1 contains a plot showing the CNR dependence on the LO power and signal power from Eq. (2). We observe that the CNR peaks at LO levels comparable to the signal levels. These values are given in the table below. If we consider the case of $N_s=100$ with $DCR=0$, we see that the asynchronous detector achieves a peak CNR value of roughly 6, whereas the peak CNR achieved with an ideal linear mode detector ($CNR = PDE \cdot \eta_{HET} N_S$) is 9. Thus CNR for the asynchronous detector is 2/3 that of the ideal detector for this specific example.

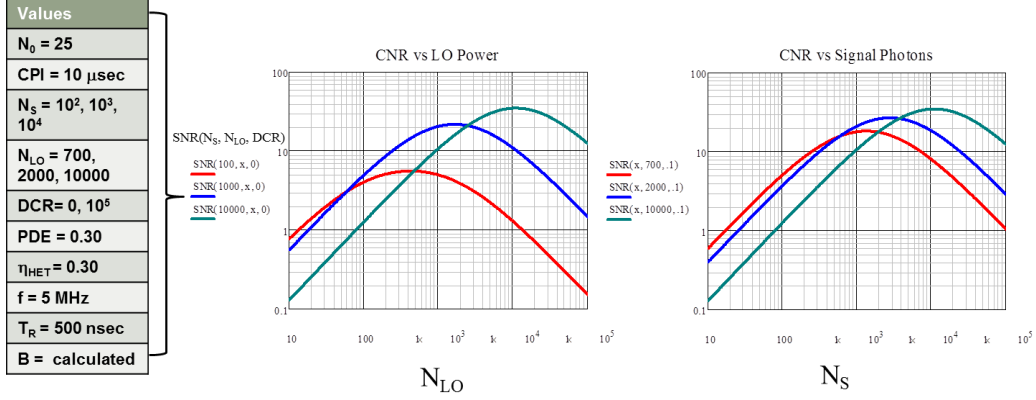


Figure 1. CNR plotted versus LO power and CNR versus signal power

2 Numerical Simulations

Here we present the results of numerical simulations performed to evaluate signal properties including the detector's frequency response and also confirm the above formulas for the blocking efficiency and CNR. We modeled the intensity of the heterodyne signal as

$$I(t) = N_S + N_{LO} + N_{DCR} + 2\sqrt{\eta_{het}}\sqrt{N_S}\sqrt{N_{LO}}\cos(2\pi ft). \quad (6)$$

This intensity signal is then used as the rate parameter for a Poisson random number generator to create the macro-pixel signal which is comprised of a series of photo-events. Figure 2 shows an example of the intensity signal, photo-events recorded by a macro-pixel and the spectrum of recorded photo-events. The parameter values used in the simulation are shown in the table on the left. The intensity signal is comprised of 50 cycles within the CPI. The corresponding photo-event stream is a vector with values given by the number of photo-events recorded by the elements of the macro-pixel as a function of time. The output of each element is filtered according to the reset time of the element. The vector is created with 1 nsec time increments. The spectrum plot shows the intensity of the two-sided Fourier transform of the signal computed from DC to 15 MHz with DC removed. The peak occurs at the input frequency of 5 MHz which exceeds the inverse reset time.

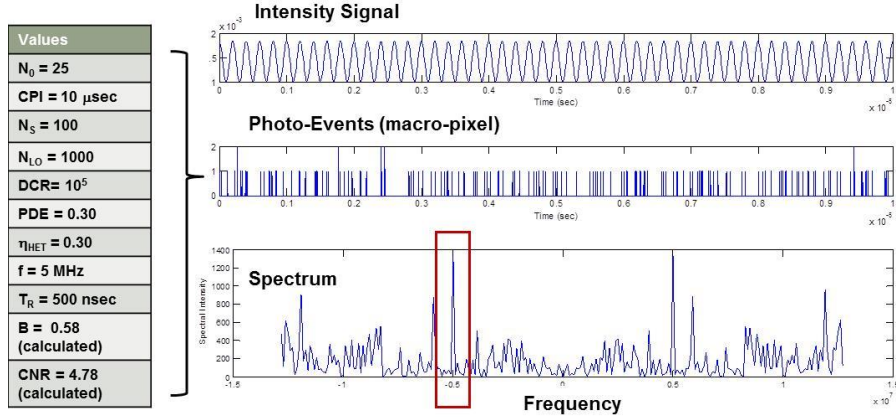


Figure 2. Example intensity signal, photo-event stream, and spectrum for the detection parameters on the left.

3 Experimental Results

The detector used in these experiments is an array of GmAPD pixels whose individual photocurrents are summed and accessible through a single connection to the array. It is a catalog part produced by SensL provided on an evaluation board with SMA connectors for bias voltage and output photocurrent.

The detector consists of 24 x 24 silicon GM pixels, and these 576 pixels comprise a single macropixel. The macropixel has a 1 x 1 mm active area with 64% fill factor, and is composed of 35 x 35 um pixels. Peak spectral response is near 440 nm.

A single source whose optical intensity was directly modulated was used to illuminate the detector. The source was a high power 405 nm LED capable of sinusoidally modulating the optical intensity between 10 and 100 MHz. The LED was collimated and it illuminated a variable aperture iris through a ground glass diffuser. The iris was then imaged onto the detector. The photocurrent was processed to produce an integer number of counts at each time sample. This data was then Fourier transformed and the spectrum was plotted. Data sets were collected at modulation frequencies of 10, 30, 50, 70, and 90 MHz. The spectrum of each data set is shown in the figure below. Modulation is clearly present in the photocurrent even at a modulation frequency of 90 MHz, although the response decreases with increasing frequency. This decrease in response may result from reduced modulation depth of the source and in future work we will monitor this with a linear mode detector. For a single pixel with a dead time of 260 ns, the fastest sampling rate possible is 3.8 MHz. This corresponds to a Nyquist frequency of 1.9 MHz (two samples per cycle). The macropixel is able to detect modulation at approximately 50 times the Nyquist frequency of a single pixel.

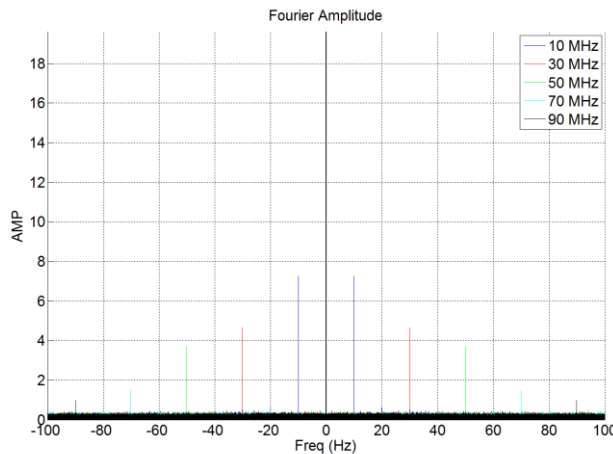


Figure 3 Several data sets overlaid. Each data set is the spectrum of detected photocurrent produced by light sinusoidally modulated at one frequency.

4 Summary

In this paper we have shown the utility of asynchronous GmAPD detector arrays for performing coherent detection in applications that require large-format, high-bandwidth detection. Results show that the performance obtained using an asynchronous GmAPD detector is always lower than that of a conventional linear mode detector. However, this loss in performance is likely offset for many applications by the large format and high sampling rates of asynchronous GmAPDs. We also performed experiments that confirm the theory and show that asynchronous GMAPDs retain frequency information well in excess of the reciprocal reset time.

References

1. J. C. Marron and M. J. Halmos, "Coherent Detection with an Asynchronous Geiger Mode Receiver," MSS Proceedings of 2014 Active E-O Systems, Springfield, VA, 2014.
2. J. X. Luu and L. A. Jiang, "Saturation effects in heterodyne detection with Geiger-mode InGaAs avalanche photodiode arrays," Appl. Opt. 45, 2006.